

# Experimental study of stress evaluation of unbonded tendon under ultimate load

Autor(en): **Mood, Jeong-Ho / Lim, Jae-Hyung / Lee, Li-Hyung**

Objekttyp: **Article**

Zeitschrift: **IABSE reports = Rapports AIPC = IVBH Berichte**

Band (Jahr): **81 (1999)**

PDF erstellt am: **22.07.2024**

Persistenter Link: <https://doi.org/10.5169/seals-61411>

## **Nutzungsbedingungen**

Die ETH-Bibliothek ist Anbieterin der digitalisierten Zeitschriften. Sie besitzt keine Urheberrechte an den Inhalten der Zeitschriften. Die Rechte liegen in der Regel bei den Herausgebern.

Die auf der Plattform e-periodica veröffentlichten Dokumente stehen für nicht-kommerzielle Zwecke in Lehre und Forschung sowie für die private Nutzung frei zur Verfügung. Einzelne Dateien oder Ausdrucke aus diesem Angebot können zusammen mit diesen Nutzungsbedingungen und den korrekten Herkunftsbezeichnungen weitergegeben werden.

Das Veröffentlichen von Bildern in Print- und Online-Publikationen ist nur mit vorheriger Genehmigung der Rechteinhaber erlaubt. Die systematische Speicherung von Teilen des elektronischen Angebots auf anderen Servern bedarf ebenfalls des schriftlichen Einverständnisses der Rechteinhaber.

## **Haftungsausschluss**

Alle Angaben erfolgen ohne Gewähr für Vollständigkeit oder Richtigkeit. Es wird keine Haftung übernommen für Schäden durch die Verwendung von Informationen aus diesem Online-Angebot oder durch das Fehlen von Informationen. Dies gilt auch für Inhalte Dritter, die über dieses Angebot zugänglich sind.





## Experimental Study of Stress Evaluation of Unbonded Tendon under Ultimate Load

Jeong-Ho Moon  
Professor, Ph.D  
Department of Architectural Engineering  
Hannam University, Taejon, Korea



Jeong-Ho Moon, born 1959.  
He received his Ph.D degree from  
University of Texas at Austin, USA.

Jae-Hyung Lim  
Director, Ph.D  
ALT Structural Research Group  
Seoul, Korea



Jae-Hyung Lim, born 1963.  
He received his Ph.D degree from  
Hanyang University, Seoul, Korea.

Li-Hyung Lee  
Director, Dr. Eng.  
advanced STructure RESearch Station  
Hanyang University, Seoul, Korea



Li-Hyung Lee, born 1941.  
He is a professor of architectural  
engineering at Hanyang University,  
Seoul, Korea. He received his Dr. Eng.  
degree from Tokyo University, Japan.

### Summary

The present study describes an experimental study for the evaluation of the unbonded tendon stress in prestressed concrete member at flexural failure. A test program with fourteen beams and slabs was planned to identify the contribution of each important variable. The variables are effective prestress, concrete strength, amount of tendons, amount of bonded reinforcements, loading type, and span/depth ratio. It was found that the tendon stress increment decreases as the level of effective prestress or amount of unbonded tendon and bonded reinforcements increases. Also, the contributions of concrete strength, and loading type were observed to affect on the tendon stresses. However, the tendon stress increments of unbonded tendon were higher than the ACI Code equation at high values of span/depth.

### 1. Introduction

The behavior of the members with unbonded tendon is different from that of the members with bonded tendon. Equilibrium and compatibility equations can be applied to the members with bonded tendon assuming that the tendon and concrete behave as a body since they are bonded completely in the member with bonded tendon. In the members with unbonded tendon, however, the tendon and concrete behave independently except at the both ends of the member. Therefore, the analysis must be based on the global compatibility rather than on the local compatibility. The latter means that the tendon and concrete behave as a body in any section of the member. The former means that the overall elongation of the concrete equals to the total lengthening of the tendon at the location of the tendon.

Many researches have been carried out as to the members with unbonded tendon, on the basis of



which various design equations such as ACI code have been proposed so far. But it is hard to say that global compatibility is fully considered in the existing code equations which have been proposed or put into use. Furthermore, those design equations are based on the very limited parameters and experiments and they generalize the data derived from the limited parameters of one or two.

The previous study<sup>(1)(2)</sup> in relation to the present study have investigated the problems of ACI code equation and of the existing design equations, on the basis of which new design equation have been proposed. The proposed design equation has been verified with the existing experimental results and compared with the existing design equations. The present paper describes the experimental study which is also aimed to verify the validity of the proposed design equation.

## 2. Test program

The number of specimens was 14 and they were designed according to ACI 318-95. The parameters for the experiment were effective prestress, concrete strength, amount of tendon, amount of bonded reinforcement, span/depth ratio, and loading type.

The span of specimens was fixed to be 4.0m to comply with the laboratory condition. The cross section was a rectangle with 20cm by 30cm. However G-series specimens had width of 60cm and depth of 12, 15, 25cm. The specimen list was illustrated in Table 1 and the details of the representative specimen (A-1) in Fig. 1.

The tendon was low relaxation 3-wire strand. The tendon was manufactured as a mono-strand in which grease was inserted in the PE pipe in a factory. Its tensile strength was around 1860 MPa Grade, main reinforcements were 8 mm diameter and stirrups were 6 mm diameter. Concrete was mixed in batch plant of PC manufacturing factory. The maximum size of aggregate was 19 mm and the design strength was 30 MPa, 40 MPa, and 60 MPa.

Table 1 Specimen list

Specimen	Loading type	$f_{se}$	$f'_c$ MPa	$\square_p$	$\square_s$	$L/d_p$
A-1	Uniform (4-point)	$0.6f_{pu}$	23.4	0.00256	0.00242	17.5
B-1		$0.7f_{pu}$	23.5			
B-2		$0.5f_{pu}$				
C-1		$0.6f_{pu}$	38.4			
C-2			52.9			
D-1			23.5	0.00171 0.00341		
D-2						
E-1			23.5	0.00256	0.00323	
E-2					0.00485	
F-1	2-point 1-point	23.5		0.00242		
F-2						
G-1	Uniform (4-point)	23.5	0.00146	0.00194	18	
G-2				0.00216	30	
G-3				0.00216	45	

\* NOTE : Tendon profile = Straight

$f_{pu}$  = 1860 MPa Grade

$f_y$  = 420 MPa Grade

$\square_6$  = 0.1982cm<sup>2</sup> (3-wire mono-strand)

D8 = 0.50cm<sup>2</sup> (Deformed bar)

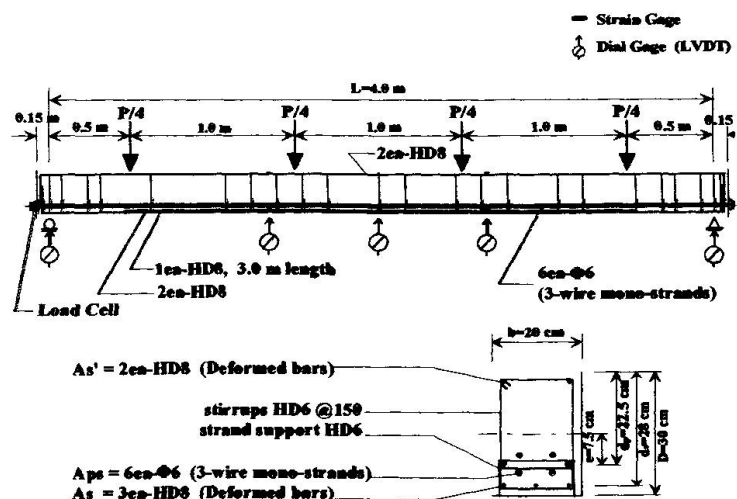


Fig. 1 Details of specimen (A-1)



### 3. Experimental results and investigations

#### 3.1 Cracking and failure patterns

The specimens were designed following the ACI code requirement of  $\square M_n > 1.2M_{cr}$  to ensure the ductile mode of failure.

As seen in Table 2, the specimens was considered to be appropriate since the ratio of maximum load to the cracking load was more than 2.0 as a whole. The vertical hair crack was initiated at the center where moment is maximum. Vertical flexural cracks spread to the support in a regular interval on both sides with the gradual increase of the load to the yielding load. After the yield load, the flexural crack did not spread beyond the range which was assumed to be plastic hinge length and new cracks emerged between the existing cracks.

In the section of maximum flexural moment, the width of cracks got wider and the flexural crack proceeded to the extreme compressive concrete fiber. From this point to the right before the maximum load, the width of 1-3 cracks got wider than that of other cracks around. When the load reached the maximum, there happened a compressive failure in the center extreme compressive concrete. After the compressive failure of the extreme compressive concrete, the capacity decreased rapidly and the deflection increased rapidly.

The cracking patterns can be explained with the curvature distribution which is related with the

Table 2 Experimental results

Specimen	$F_{se}$ (kN)	$F_{ps}$ (kN)	$\square F_{ps}$ (kN)	$P_{cr}$ (kN)	$P_{max}$ (kN)	$P_{max}/P_{cr}$	$\square_{max}$ (mm)
A-1	22.25	32.93	10.68	57.33	124.66	2.17	73.8
B-1	25.77	34.79	9.02	55.86	118.58	2.12	72.8
B-2	18.82	32.14	13.32	44.59	114.17	2.56	90.2
C-1	21.85	33.42	11.57	56.84	119.27	2.09	74.8
C-2	22.15	35.67	13.52	61.74	131.03	2.12	97.6
D-1	22.25	35.87	13.62	40.18	95.55	2.37	97.4
D-2	22.15	32.14	9.99	59.78	138.77	2.32	69.2
E-1	22.15	32.83	10.68	52.92	120.05	2.26	74.0
E-2	21.95	28.81	6.86	55.86	132.69	2.37	48.8
F-1	22.05	33.04	10.99	40.18	78.92	1.96	97.4
F-2	22.05	31.75	9.70	27.44	55.27	2.01	71.8
G-1	22.05	36.95	14.90	100.9	228.44	2.26	122.4
G-2	22.05	32.63	10.58	34.01	66.05	1.94	118.4
G-3	22.05	32.34	10.29	15.78	31.07	1.96	166.6

$F_{se}$  : Effective prestress/1ea       $P_{max}$  : Maximum load

$F_{ps}$  : Ultimate tendon stress/1ea       $P_{cr}$  : Initial cracking load

$\square F_{ps}$  : Tendon stress increase/1ea       $\square_{max}$  : Maximum deflection

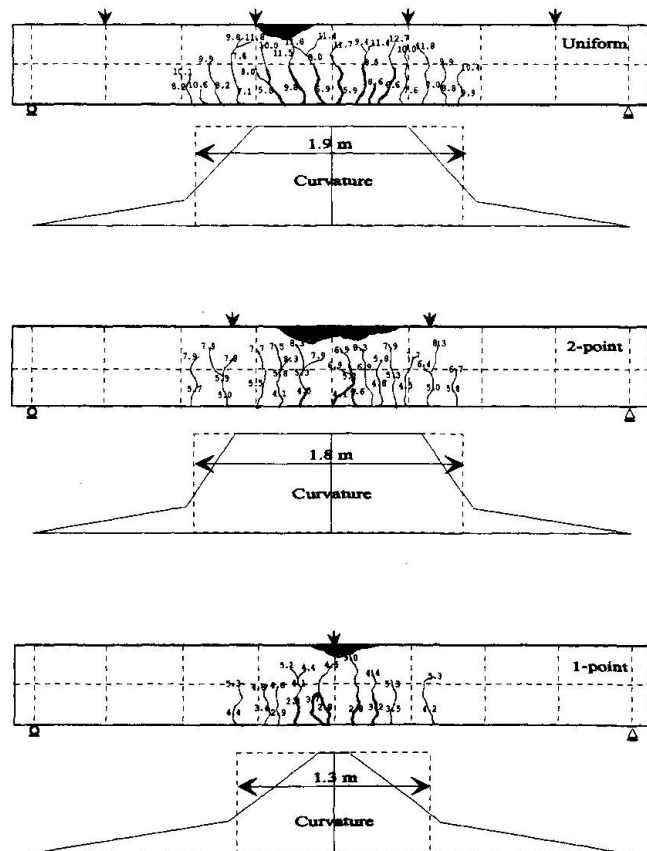


Fig. 2 Final failure pattern depending on type of applied load

type of applied load. Fig. 2 illustrates the final failure patterns of one of specimens. The plastic hinge lengths under 2-point load or uniform load (4-point load) were almost same since the ranges of the cracks under 2-point load or uniform load were 1.8m and 1.9m, respectively. In case of 1-point load, however, the range of cracking was 1.3m, which was smaller than the cases of 2-point load or uniform load.

### 3.2 Parametric effects

The unbonded tendon stress were computed with the prediction equations<sup>(2)(4)</sup>. The results were illustrated in Fig. 3 to 8. The meaning of the abbreviations used in the figures are as follows.

- Exp = The experimental results
- Compatibility<sup>(2)</sup> = Strain compatibility method
- ACI<sup>(4)</sup> = ACI 318-95 equation
- Design<sup>(2)</sup> = design equation proposed by authors

The computed results by strain compatibility method were compared with experimental results. The design equation proposed by authors was also examined. Those tested and computed tendon stresses were also compared with the current ACI Code equation. Followings were the description the effect of each parameter.

#### (1) Effective prestress ( $f_{se}$ )

Fig. 3 shows a comparison between the computed results and the experimental results for the tendon stress increases depending on the level of effective prestresses. As seen from the figure, the experimental results agree well with the computed results by the strain compatibility method. It means that the computational model of the strain compatibility method is accurate to evaluate the ultimate stress of unbonded tendon. The experimental results show that the tendon stress increases are decreasing as the level of effective prestress increases. But the current ACI Code equation predicted to remain constant regardless of the level of the effective prestresses. The ultimate stresses of the tendon were underestimated up to 68%-83% of the experimental values. The results by the design equation by authors was the same as in the tendency of the experiment results. As increases the effective prestress, the tendon stress at failure decreases. The ultimate stresses of the tendon ( $f_{ps}$ ) turns out to be 77%-87% of the experimental values which provides better predictions compared with the current ACI Code equation.

#### (2) Concrete strength ( $f'_c$ )

Fig. 4 shows a comparison between the results of computation and experiment at variation of

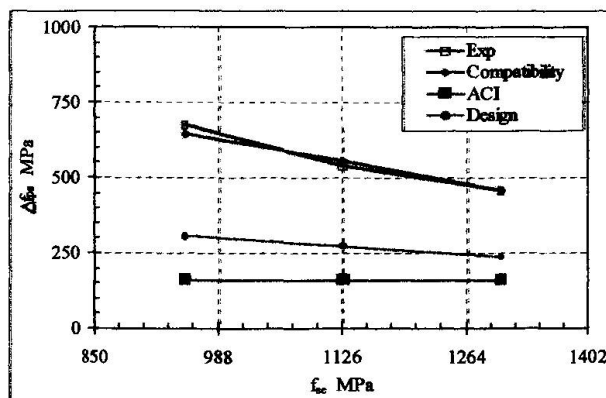


Fig. 3 Effect of effective prestress

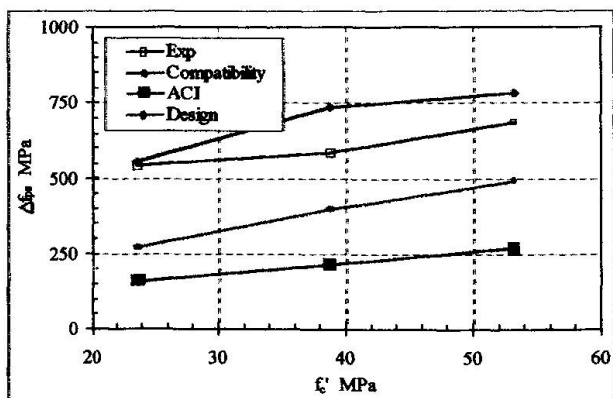


Fig. 4 Effect of concrete strength



concrete strengths. As seen in the figure, with the increase of concrete strength, tendon stress increase has a tendency to rise in all the results of the experiment, the proposed design equation, and the current ACI Code equation. But they differ in the type of tendon stress increase: the tendon stress increase is in the linear shape in the result of the current ACI Code equation whereas it is not in the results of experiment and the proposed design equation. Because the proposed design equation contains the term  $f_c'/\square_p$  which is the same parameter as in the ACI Code equation but in the form of a square root.

### (3) Amount of tendon ( $A_{ps}$ )

Fig. 5 shows a comparison of the results of computation and experiment depending on the change of the amount of the tendon. The experimental results coincide well with the results by the strain compatibility method. As the amount of tendon increases, the tendon stress increase shows a nonlinear shape variation in all computed results and experimental results. Thus, it can be said that both the ACI Code equation and the proposed design equations consider the amount of tendon accurately to predict the ultimate stress of unbonded tendon. The difference is that the ACI Code equation underestimates the ultimate stress of the tendon with the range of 73%-77% of the experimental value whereas the proposed design equation predicted it to be 82% of the experimental values.

### (4) Amount of reinforcement ( $A_s$ )

Fig. 6 compares the results of computation and experiment depending on the change of the amount of reinforcement. As is known in the figure, with the increase of amount of reinforcement, tendon stress increase decreases in computations and experiment. However, ACI Code equation evaluates it with no variations. It is because the current ACI Code equation does not consider the effect of the amount of reinforcement. Since the amount of reinforcement makes an influence on the ultimate stress of unbonded tendon as seen in the experimental results, it is better to consider the amount of reinforcement as a variable like the proposed design equation.

### (5) Loading type ( $f$ , $L_o/L=1/f+L/d_p$ )

The results of the computation and the experiment were compared in Fig. 7 in which the loading types were varied. As seen from the experiments, the tendon stress increases were observed to have similar values in cases of uniform load (4-point load) and 2-point load. As in the proposed design equation, therefore, it is possible to use an identical coefficient for the loading types of the uniform load and 2-point load. However the experimental result for an 1-point load showed smaller tendon stress than those of uniform load and 2-point load. Thus it can be concluded that the loading type affects the ultimate stress of unbonded tendon.

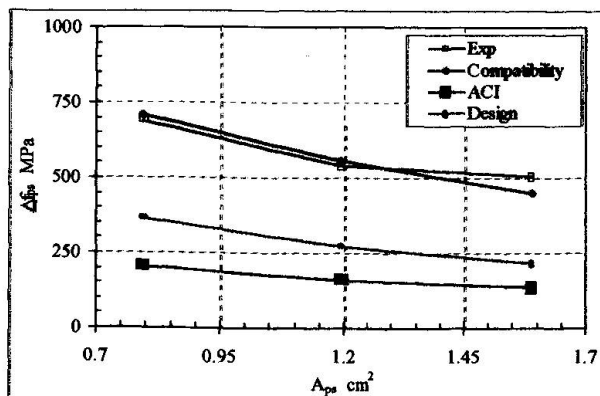


Fig. 5 Effect of amount of tendon

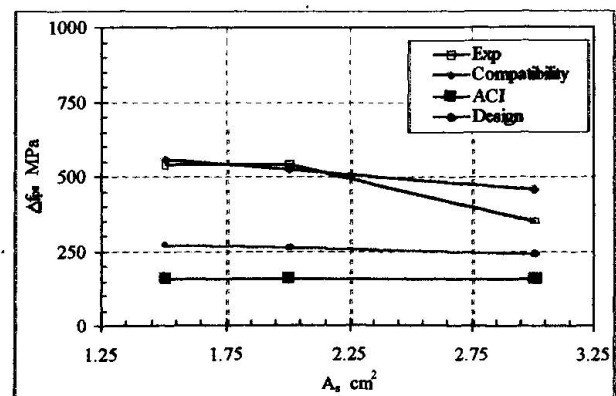


Fig. 6 Effect of amount of reinforcement

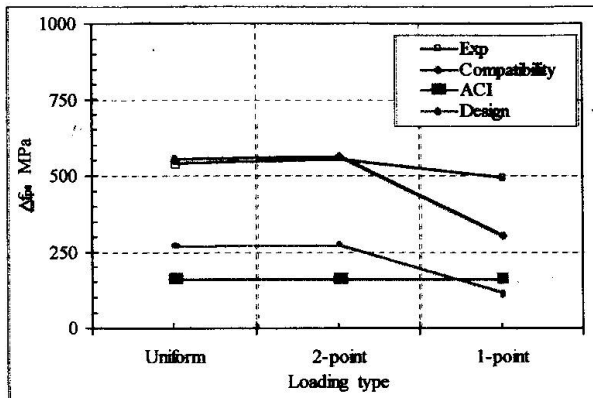


Fig. 7 Effect of loading type

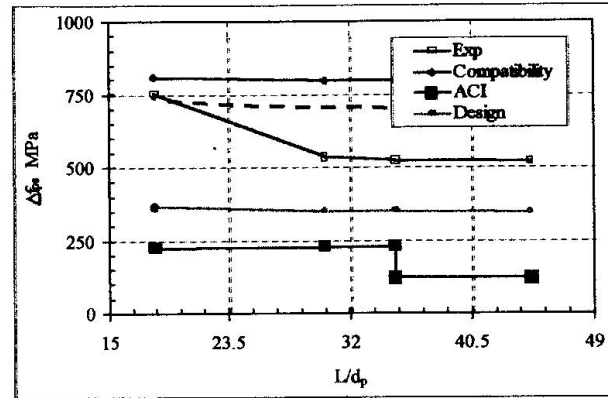


Fig. 8 Effect of span/depth ratio

#### (6) Span/depth ratio ( $L/d_p$ )

Fig. 8 illustrates a comparison between the results of the computation and the experiment depending on the change of span/depth ratio. As is clear in the figure, the stress increase of unbonded tendon decreases when the span/depth ratio is less than 30, but it regularly increases when the ratio is greater than 30. However, the results by the proposed design equation predicted almost uniform values. It is because the function of plastic hinge length ratio is made by the combination of the loading type and span/depth ratio in the proposed equation<sup>(2)</sup>. It exhibits a minor influence of the change of the span/depth ratio on the ultimate stress of unbonded tendon when the ratio is over 15, and the ultimate stress of unbonded tendon is influenced more by the loading type rather than by the effect of the span/depth ratio. However, the difference between the results of the strain compatibility method and the experiment is due to the fact that the measurement of deflections was stopped since the capacity of the experimental equipment was over. If the experiment was continued up to the final failure, the tendon stress increase would be the curve shown with the dotted line.

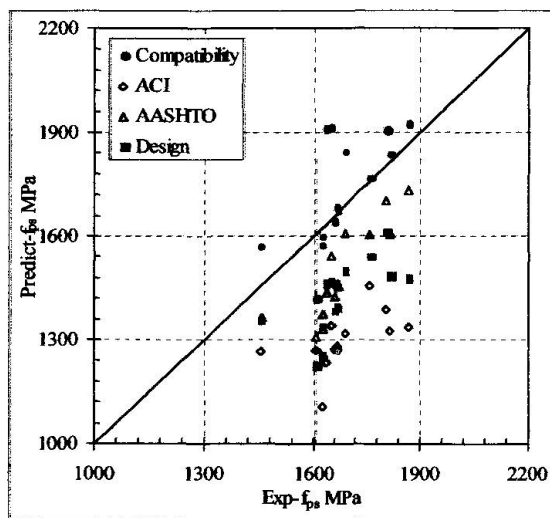
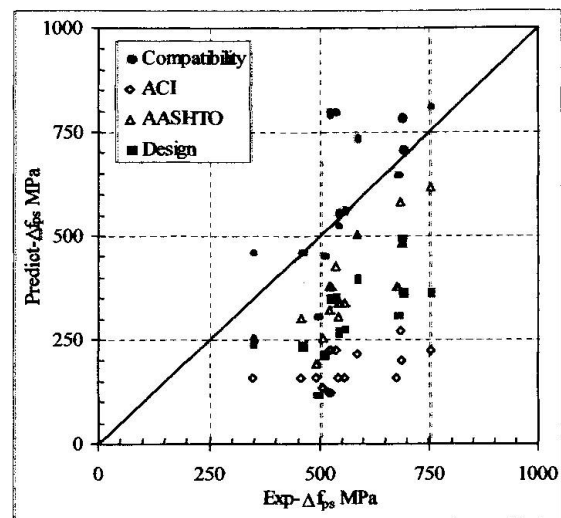
### 4. Evaluation of proposed design equation

The mean value and standard deviation of the ratio of the prediction to the experiment are illustrated in Table 3 and the comparisons of  $f_{ps}$  and  $\square f_{ps}$  are shown in Fig. 9. The probable reliance is considered to be good if the average of predicted value/experimental value ( $f_{psp}/f_{pse}$ ) ratio is higher and standard deviation is smaller. It is also said that the predictions are reliable if the makers in Fig. 9 are close to the line of perfect correlation. As the table and figure indicate, the results by the strain compatibility method (Compatibility) predict accurately the ultimate stress of unbonded tendon since predicted value/experimental value is 1.01 at  $f_{ps}$ , 1.03 for  $\square f_{ps}$ .

The proposed design equation can predict the ultimate stress of unbonded tendon more accurately than the ACI Code equation. When compared with the previous design equations, the proposed design equation predicted the tendon stress values which were a little bit less than AASHTO LRFD Code equation. However, the proposed design equation shows a better

Table 3 Average value and standard deviation of predicted value/experimental value ( $f_{psp}/f_{pse}$ ) ratio

Items	$f_{psp}/f_{pse}$ Ratio		$\square f_{psp}/\square f_{pse}$ Ratio	
	Mean values	Standard deviations	Mean values	Standard deviations
Compatibility	1.01	0.086	1.03	0.286
ACI	0.77	0.081	0.35	0.155
AASHTO	0.88	0.069	0.63	0.184
Harajli/Kanj	0.83	0.074	0.51	0.185
Chakrabarti	0.85	0.086	0.58	0.255
Design	0.84	0.058	0.53	0.166

Fig. 9(a) Comparisons of  $f_{ps}$ Fig. 9(b) Comparisons of  $\Delta f_{ps}$ 

standard deviation. Further AASHTO LRFD Code equation is not suitable for a design purpose because a complex computational procedure is needed to solve a quadratic equation.

## 5. Conclusions

- (1) The tendon stress increment decreases as the effective prestress increases.
- (2) The parameters of concrete strength, amount of tendons and bonded reinforcements, and loading type were observed to affect on the tendon stresses.
- (3) The tendon stress increments were higher than the ACI Code equation at high values of span/depth.
- (4) The strain compatibility method can predict accurately the stress of unbonded tendon.
- (5) The design equation proposed by the authors can predict the tendon stress accurately with an appropriate safety margin.

## Acknowledgment

The authors would like to thank STRESS (advanced STructure RESearch Station) at Hanyang University and Kumho Construction & Engineering Co., Ltd. for providing financial support for this study.

## References

1. Jae-Hyung Lim, Jeong-Ho Moon, Seong-Woo Eum, Li-Hyung Lee, "Evaluation of ultimate stress of unbonded tendon in prestressed concrete members(I) -Consideration of ACI code and state-of-art-." Journal of Korea Concrete Institute, Vol. 9 No. 4, Aug., 1997, pp 167-176.
2. Jae-Hyung Lim, Jeong-Ho Moon, Seong-Woo Eum, Li-Hyung Lee, "Evaluation of ultimate stress of unbonded tendon in prestressed concrete members(II) -Proposed design equation using strain compatibility-." Journal of Korea Concrete Institute, Vol. 9 No. 5, Oct., 1997, pp 105-114.
3. Jae-Hyung Lim, Li-Hyung Lee, "Effect of influential factors on the ultimate stress of





- unbonded post-tensioning tendon." Journal of Architectural Institute of Korea, Vol. 13 No. 10, Oct., 1997, pp 291-300.
4. ACI Committee 318, "Building Code Requirements for Structural Concrete (ACI 318-95) and Commentary (ACI 318R-95)", American Concrete Institute, Farmington Hills, MI, 1995, 369 pp.
  5. Chakrabarti, P. R., "Ultimate stress for unbonded post-tensioning tendons in partially prestressed beams." ACI Journal, Nov.-Dec., 1995, pp 689-697.
  6. ACI-ASCE Committee 423, "Recommendations for concrete members prestressed with unbonded tendon." ACI Journal, May-June, 1989, 18 pp.
  7. Harajli, M. H., and Kanj, M. Y., "Ultimate flexural strength of concrete members prestressed with unbonded tendons." ACI Journal, Vol. 88, No. 6, 1991, pp 663-673.
  8. Naaman, A. E., and Alkhairi, F. M., "Stress at ultimate in unbonded post-tensioning tendons. Part II: Proposed methodology." ACI Journal, Nov.-Dec., 1991, pp 683-692.